Sub-Doppler light amplification in a coherently pumped atomic system

Yifu Zhu and Jun Lin
Department of Physics, Florida International University, Miami, Florida 33199
(Received 8 May 1995)

We report the observation of steady-state amplification of a weak probe laser without population inversion in the bare states in a Doppler-broadened Λ-type Rb atomic system. The probe amplification was observed with the Rabi frequency of a coupling laser much smaller than the Doppler width and can be viewed as due to the dressed-state inversion. A 10% single-pass amplification of a weak probe laser was obtained, and the measured linewidth of the gain spectral feature approaches the Rb natural linewidth. A theoretical analysis based on a three-level Doppler-broadened Λ system is presented, and qualitative agreement with the experiment results is achieved.

PACS number(s): 42.50.Gy, 42.50.Hz, 32.90.+a, 32.70.Jz

I. INTRODUCTION

Quantum coherence and interference among atomic states coupled by laser fields provide a variety of phenomena for fundamental study and offer possibilities for practical applications. There have been many theoretical proposals for manipulating atomic coherence to achieve light amplification without population inversion [1–6]. Laser action related to a noninverted population in a strongly pumped two-level system has been demonstrated before [7–9]. Recent studies have focused on the laser-induced coherence in multilevel systems because of their potential usefulness in generating laser light in the electromagnetic spectral regions where lasing with population inversion is difficult to achieve. There have been several interesting experiments demonstrating light amplification without inversion in the time-dependent transient regime [10–13]. Recently, steady-state inversionless gain in a strongly pumped four-level Raman system [14] with collisional energy transfer has been reported [15]. While a common term, lasing without population inversion (LWI), is used to describe the properties of light amplification in these systems, the origin of gain may be different in distinct cases.

Generally speaking, LWI may be classified into two categories: first, LWI in any state basis; second, LWI in the bare atomic states, but with inversion in a hidden-state basis, such as dressed states. Usually one can distinguish the two cases from the spectrum of the gain line profile and the pumping scheme. For LWI in any state basis, a strong coupling laser generally is near resonance with the atomic transition, and the gain feature appears at the line center of another atomic transition (without the coupling laser, the line center corresponds to the maximum absorption) [16,21]. For LWI in the bare atomic states, but with inversion in the dressed states, the strong-coupling laser normally is detuned from the atomic transition while the gain feature on the other atomic transition occurs at one of the Autler-Townes doublet transitions [17,20,21]. The resulting gain and/or absorption spectrum is asymmetrical.

Here we present an experimental study of steady-state light amplification in a three-level Λ system, similar to that theoretically studied by Imamoglu *et al.* [16]. The experiment was carried out in a Doppler-broadened Rb atomic sample driven by an off-resonance coupling laser. We obtained 10% amplification of a weak probe laser and observed a sub-Doppler linewidth in the gain spectral profile. The observed sub-Doppler probe amplification can be viewed as LWI in the bare atomic states, but with inversion in the dressed states.

II. EXPERIMENTAL RESULTS

The Rb three-level Λ system is realized with the laser-coupled D_2 transitions and is depicted in Fig. 1. A coupling laser connects the Rb $5S_{1/2}$ ($F=2$ for ^{85}Rb atoms or $F=1$ for ^{87}Rb atoms)$\leftrightarrow 5P_{3/2}$ transition, and a probe laser couples the Rb $5P_{3/2}\leftrightarrow 5S_{1/2}$ ($F=3$ for ^{85}Rb atoms or $F=2$ for ^{87}Rb atoms) transition. A resonant pump laser is applied to the Rb $5S_{1/2}$ ($F=3$ for ^{85}Rb atoms or $F=2$ for ^{87}Rb atoms) $\leftrightarrow 5P_{3/2}$ transition and excites the atoms to the Rb $5P_{3/2}$ excited state. The atomic coherence ρ_{12} between the two ground hyperfine states of ^{85}Rb atoms, $5S_{1/2}$ $F=3$ and $F=2$ (or $5S_{1/2}$ $F=2$ and $F=1$ states for ^{87}Rb atoms), is induced by the coupling laser and the probe laser. When the pump laser excites some Rb atoms to the $5P_{3/2}$ state, the probe laser can be amplified by the atomic coherence ρ_{12} even though there is no population inversion between the excited state $5P_{3/2}$ and the ground states $5S_{1/2}$.

The experimental apparatus is shown schematically in Fig. 2. The experiment was done in a 75-mm natural Rb vapor cell operating at temperatures up to 60 °C. A cw single-frequency Ti:sapphire laser (Coherent Model No. 899-21) was used as the coupling laser, and a cw external-cavity diode laser and a cw temperature-stabilized diode laser were

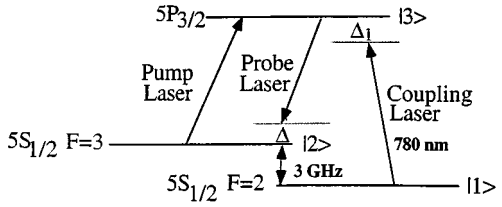

FIG. 1. Coherently pumped ^{85}Rb three-level Λ system. Δ_1 (Δ) is the pump (probe) detuning. For ^{87}Rb atoms, the ground hyperfine states are $5S_{1/2}$ $F=2$ and $5S_{1/2}$ $F=1$.

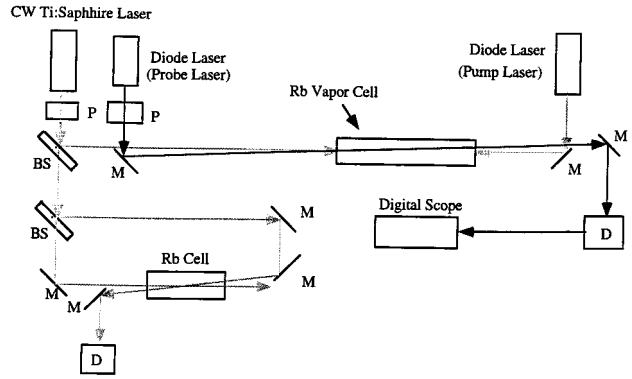

FIG. 2. Schematic drawing of the experiment. *M* stands for a mirror, BS for a beam splitter, *P* for a polarizer, and *D* for a photodetector.

used as the probe and pump lasers, respectively. The coupling laser and the probe laser had linear orthogonal polarizations and propagated in the same direction, opposite to that of the pump laser. The three laser beams were overlapped in the Rb cell with a relative angle of about 3×10^{-3} rad. After passing through the Rb cell, the probe-laser beam was directed to a photodiode, and its output was recorded by a digital oscilloscope (Lecroy Model No. 9310A) and the data were stored in a personal computer for later analysis. A simultaneous saturation absorption experiment was used as a frequency calibration for the Ti:sapphire laser. The coupling laser and the pump laser both had a beam diameter of about 1.5 mm, while the beam diameter for the probe laser was about 1 mm. The probe-laser power was kept below 1 μW, the pump-laser power was about 0.2 mW, and the coupling laser power was varied between 700 and 1 mW. During the experiment, the coupling-laser frequency and the pump-laser frequency were fixed at appropriate detunings from the corresponding Rb transitions, while the probe laser was scanned across the Rb $5S_{1/2}\leftrightarrow5P_{3/2}$ transition, and the probe-laser absorption and/or gain spectrum was recorded.

Figure 3 shows the probe absorption and/or gain spectrum recorded with the coupling laser power at 50 mW for the D_2 transitions of both Rb isotopes, ^{85}Rb and ^{87}Rb (the isotope shift is 1.125 GHz and abundance is 72.17% and 27.83%, respectively). Curve 1 in Fig. 3(a) is the probe absorption spectrum recorded without both the coupling laser and the pump laser, and the Rb cell is at room temperature. It displays the ^{87}Rb $5S_{1/2}$ $(F=2)\leftrightarrow5P_{3/2}$ transition at $\Delta=-1.125$ GHz and the ^{85}Rb $5S_{1/2}$ $(F=3)\leftrightarrow5P_{3/2}$ transition at $\Delta=0$. Curves 2 and 3 in Fig. 3(a) are the probe spectra recorded at the Rb cell temperature 60 °C with both the pump laser and coupling laser on. For curve 2, the coupling laser was blue detuned ($\Delta_1=1.4$ GHz) from the ^{85}Rb $5S_{1/2}$ $(F=2)\leftrightarrow5P_{3/2}$ transition, and the pump laser was tuned to the Doppler-broadened ^{85}Rb $5S_{1/2}$ $(F=3)\leftrightarrow5P_{3/2}$ transition. The probe laser experiences about 10% amplification at the probe detuning $\Delta\approx1.4$ GHz from the ^{85}Rb $5S_{1/2}$ $(F=3)\leftrightarrow5P_{3/2}$ transition. The probe amplification from the ^{87}Rb atoms near the ^{87}Rb $5S_{1/2}$ $(F=2)\leftrightarrow5P_{3/2}$ transition ($\Delta\approx-1.2$ GHz) is shown by curve 3, in which the coupling laser was red detuned ($\Delta_1=-1.2$ GHz) from the ^{87}Rb $5S_{1/2}$ $(F=1)\leftrightarrow5P_{3/2}$ transition while the pump laser was tuned to the ^{87}Rb $5S_{1/2}$ $(F=2)\leftrightarrow5P_{3/2}$ transition. Figure 3(b) shows the probe-laser amplification by the coherently pumped ^{85}Rb atoms on an expanded scale and demonstrates the effect of the pump laser. The dashed curve was recorded when the pump laser was blocked, while the solid

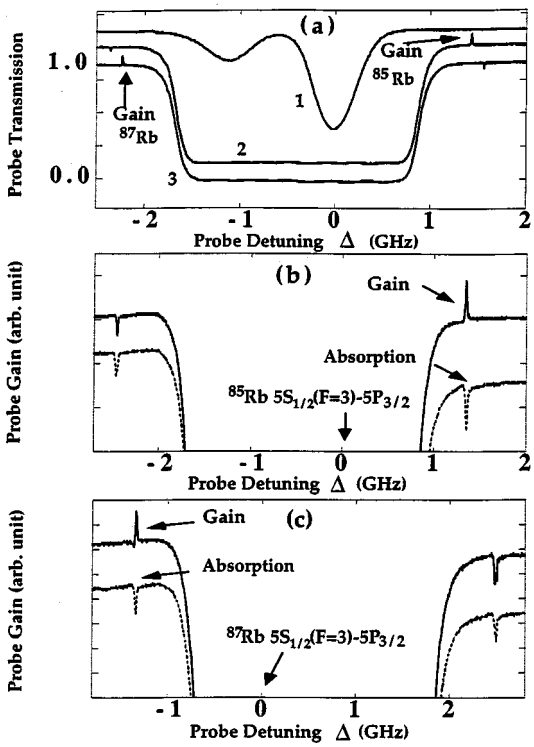

FIG. 3. (a) Curve 1: the probe transmission spectrum with the Rb cell at room temperature and without the coupling laser and the pump laser. The horizontal scale is the probe detuning from the ^{85}Rb $5S_{1/2}$ $(F=3)\leftrightarrow5P_{3/2}$ transition. The absorption peak at $\Delta=-1.125$ GHz corresponds to the ^{87}Rb $5S_{1/2}$ $(F=2)\leftrightarrow5P_{3/2}$ transition while the peak at $\Delta=0$ corresponds to the ^{85}Rb $5S_{1/2}$ $(F=3)\leftrightarrow5_{3/2}$ transition. Curves 2 and 3 are the probe transmission spectra with the Rb cell at 60 °C. For curve 2, the coupling laser is detuned from the ^{85}Rb $5S_{1/2}$ $(F=2)\leftrightarrow5P_{3/2}$ transition by $\Delta_1=1.4$ GHz and the pump laser is tuned to the center of the Doppler-broadened ^{85}Rb $5S_{1/2}$ $(F=3)\leftrightarrow5P_{3/2}$ transition. The recorded probe gain at $\Delta\approx\Delta_1=1.4$ GHz is about 10%. Curve 3 is the probe spectrum recorded with the pump detuning $\Delta_1=-1.2$ GHz from the ^{87}Rb $5S_{1/2}$ $(F=1)\leftrightarrow5P_{3/2}$ transition, and the pump laser is tuned to the center of the ^{87}Rb $5S_{1/2}$ $(F=2)\leftrightarrow5P_{3/2}$ transition. The probe gain occurs at $\Delta\approx\Delta_1=-1.2$ GHz [$\Delta\approx-2.2$ GHz in the horizontal scale measured from the ^{85}Rb $5S_{1/2}$ $(F=3)\leftrightarrow5P_{3/2}$ transition]. (b) An expanded view of the measured probe absorption and/or gain spectra recorded at the Rb cell temperature 50 °C. The solid (dashed) curve was recorded with (without) the pump laser. The pump laser was tuned to the center of the ^{85}Rb $5S_{1/2}$ $(F=3)\leftrightarrow5P_{3/2}$ transition and the coupling laser was detuned from the ^{85}Rb $5S_{1/2}$ $(F=2)\leftrightarrow5P_{3/2}$ transition by $\Delta_1=1.3$ GHz. The probe exhibits gain at $\Delta\approx1.3$ GHz with the pump laser on and absorption with the pump laser off. (c) An expanded view of the measured probe absorption and/or gain spectra for the ^{87}Rb atoms at temperature 50 °C. The solid (dashed) curve was recorded with (without) the pump laser. The pump laser was tuned to the center of the ^{87}Rb $5S_{1/2}$ $(F=2)\leftrightarrow5P_{3/2}$ transition and the coupling laser was detuned from the ^{87}Rb $5S_{1/2}$ $(F=1)\leftrightarrow5P_{3/2}$ transition by $\Delta_1=-1.4$ GHz. The probe exhibits gain at $\Delta\approx-1.4$ GHz with the pump laser on and absorption with the pump laser off. For clarity, different curves have been vertically displaced.

curve was recorded with the pump laser on. Without the pump laser, no probe amplification was observed: the dominant probe absorption occurs at the line centers of the ^{85}Rb $5S_{1/2}$ $(F=3)\leftrightarrow 5P_{3/2}$ and the ^{87}Rb $5S_{1/2}$ $(F=2)\leftrightarrow 5P_{3/2}$ transitions with a Doppler-broadened line profile, while a sub-Doppler absorption profile was observed at the probe detuning approximately equal to the pump detuning $(\Delta\approx\Delta_1)$. When the pump laser was tuned to the Doppler-broadened ^{85}Rb $5S_{1/2}$ $(F=3)\leftrightarrow 5P_{3/2}$ transition, the absorption peak at $\Delta\approx 1.3$ GHz from the ^{85}Rb $5S_{1/2}$ $(F=3)\leftrightarrow 5P_{3/2}$ transition in the dashed curve is turned into the gain peak, while the sub-Doppler absorption feature (from the ^{87}Rb atoms) at the detuning -1.3 GHz from the ^{87}Rb $5S_{1/2}$ $(F=2)\leftrightarrow 5P_{3/2}$ transition ($\Delta\approx -2.4$ GHz in the horizontal scale) is not affected, as shown by the solid curve in Fig. 3(b). Figure 3(c) shows the probe laser amplification by the coherently pumped ^{87}Rb atoms on an expanded scale when the pump laser was tuned to the ^{87}Rb $5S_{1/2}$ $(F=2)\leftrightarrow 5P_{3/2}$ transition. When the pump laser was blocked, only the absorption features were recorded, as shown by the dashed line in Fig. 3(c). When the pump laser was on, the absorption peak at $\Delta\approx -1.4$ GHz for the ^{87}Rb transition $5S_{1/2}$ $(F=2)\leftrightarrow 5P_{3/2}$ is turned into the gain peak. The probe amplification was observed with the estimated Rabi frequency of the coupling laser ($\sim$120 MHz) much smaller than the Doppler width ($\sim$500 MHz), and the probe absorption and/or gain spectral feature at $\Delta\approx\Delta_1$ exhibits a sub-Doppler linewidth [the measured linewidth of the probe absorption and/or gain peaks at $\Delta\approx\Delta_1$ is about 10 MHz and is comparable to the natural linewidth of about 6 MHz for the ^{85}Rb $5S_{1/2}$ $(F=3)$ or ^{87}Rb $5S_{1/2}$ $(F=2)\leftrightarrow 5P_{3/2}$ transition]. We note that the sub-Doppler linewidth in the probe absorption feature was observed without the pump laser, and the sub-Doppler probe gain was observed when the pump laser was tuned within the Doppler-broadened Rb absorption line. The effect of the pump laser indicates that the probe amplification requires the real atomic population in the excited state.

III. THEORETICAL ANALYSIS

To understand our experimental observation, we have analyzed theoretically the three-level Λ system [16] depicted in Fig. 1. We solve the density-matrix equations of motion for the Λ system driven by a coupling laser on the $|3\rangle\leftrightarrow|1\rangle$ transition and incoherently pumped with a rate Γ (the pump laser linewidth is about 30 MHz, greater than the Rb D_2 linewidth of 6 MHz; therefore it can be approximately treated as an incoherent pump source). Under the electric-dipole and the rotating-wave approximations, the density-matrix equations can be written as

$$\dot{\rho}_{11}=-\gamma_{31}\rho_{33}+i\Omega(\rho_{31}-\rho_{13}),$$

$$\dot{\rho}_{33}=\Gamma\rho_{11}-(\Gamma+\gamma_{32}+\gamma_{31})\rho_{33}+i\Omega(\rho_{13}-\rho_{31})+ig(\rho_{23}-\rho_{32}),$$

$$\dot{\rho}_{12}=-[\Gamma/2+i(\Delta_1-\Delta)]\rho_{12}-ig\rho_{13}+i\Omega\rho_{32}, \qquad (1)$$

$$\dot{\rho}_{13}=-[\Gamma+\gamma_{32}/2+\gamma_{31}/2+i\Delta_1]\rho_{13}-ig\rho_{12}+i\Omega(\rho_{33}-\rho_{11}),$$

$$\dot{\rho}_{23}=-[\Gamma/2+\gamma_{32}/2+\gamma_{31}/2+i\Delta]\rho_{23}-i\Omega\rho_{21}+ig(\rho_{33}-\rho_{22}),$$

together with the equations of their complex conjugates. Here γ_{ij} $(i,j=1-3)$ are the radiative decay rates from state $|i\rangle$ to state $|j\rangle$ and Ω (g) is the Rabi frequency of the coupling laser (the probe laser). In a closed three-level Λ system, we have $\rho_{11}+\rho_{22}+\rho_{33}=1$. For the convenience of the calculation, Ω and g are chosen to be real quantities. The probe gain and/or absorption coefficient is proportional to $\mathrm{Im}(\rho_{23})$. In our notation, when $\mathrm{Im}(\rho_{23})>0$, the probe will be amplified while when $\mathrm{Im}(\rho_{23})<0$, the probe will be attenuated. The general steady-state solution to Eqs. (1) can be readily derived analytically (for the analysis with a resonant coupling laser, see Ref. [16]), but the tedious expressions for the solution corresponding to the situation of an off-resonant coupling laser offers no clear physical insight. We therefore opted to present the numerical calculation here. Shown in Fig. 4 are the calculated gain coefficient $[\mathrm{Im}(\rho_{23})]$ of a weak probe laser in a homogeneous Λ system plotted versus the probe detuning Δ for several coupling-laser detunings Δ_1. It is seen that for a given Rabi frequency $\Omega=20\gamma_{32}$, the probe absorption occurs at the transitions of the Autler-Townes doublet, i.e.,

$$\Delta\approx\frac{\Delta_1}{2}\pm\frac{\sqrt{\Delta_1^2+4\Omega^2}}{2}.$$

With the coupling laser detuning $\Delta_1=50\gamma_{32}$, the weak sideband at

$$\Delta\approx\frac{\Delta_1}{2}+\frac{\sqrt{\Delta_1^2+4\Omega^2}}{2}$$

is absorptive. At $\Delta_1=60\gamma_{32}$, the probe laser experiences a dispersive-type gain and/or absorption line profile at

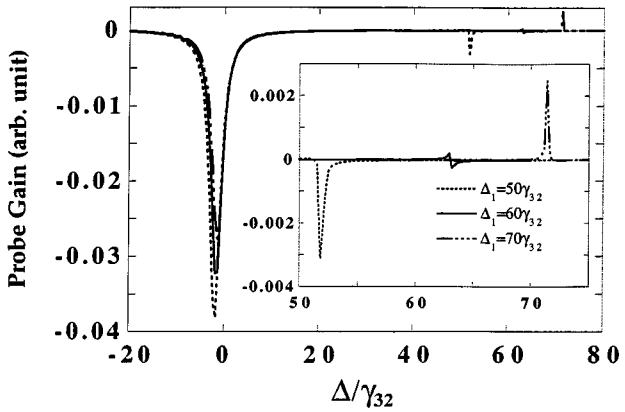

FIG. 4. Calculated probe gain and/or absorption spectra versus the probe detuning Δ for a homogeneous three-level Λ system. The chosen parameters are $\Omega=20\gamma_{32}$, $\gamma_{31}=1.1\gamma_{32}$, $\Lambda=0.1\gamma_{32}$, and the probe Rabi frequency $g=0.1\gamma_{32}$. (γ_{32} is the spontaneous decay rate from $|3\rangle\rightarrow|2\rangle$.) The inset shows the expanded view around $\Delta\approx\Delta_1/2+\sqrt{\Delta_1^2+4\Omega^2}/2$. Note that as Δ_1 increases, the spectral feature evolves from the absorption to dispersive response, then to the amplification.

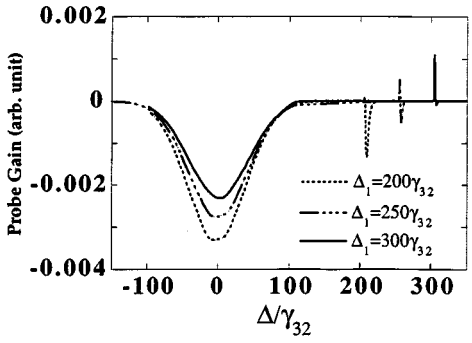

FIG. 5. Calculated probe absorption and/or gain spectra for the Doppler-broadened Λ system depicted in Fig. 1. The Doppler width is $100\gamma_{32}$, the Rabi frequency of the pump (probe) laser is $30\gamma_{32}$ $(0.1\gamma_{32})$, and the rest of the parameters are the same as that in Fig. 4. When the pump detuning Δ_1 increases from $200\gamma_{32}$ to $300\gamma_{32}$, the spectral line shape at $\Delta=\Omega'\approx\Delta_1$ evolves from absorption to dispersion, and then to amplification.

$$\Delta\approx\frac{\Delta_1}{2}+\frac{\sqrt{\Delta_1^2+4\Omega^2}}{2}.$$

Further increases of Δ_1 lead to the probe amplification at

$$\Delta\approx\frac{\Delta_1}{2}+\frac{\sqrt{\Delta_1^2+4\Omega^2}}{2}$$

as shown by the curve with $\Delta=70\gamma_{32}$. As expected, approximately at the line center of the probe transition,

$$\Delta\approx\frac{\Delta_1}{2}-\frac{\sqrt{\Delta_1^2+4\Omega^2}}{2},$$

the probe laser experiences dominant absorption. As will be discussed in Sec. IV, the probe spectrum can be understood in terms of a physical picture of dressed states. Taking the atomic velocity distribution as conventional Maxwellian and considering the Doppler cancellation configuration of the copropagating coupling laser and probe laser, we further carried out calculations for a Doppler-broadened Λ system, and the results are plotted in Fig. 5. When the coupling-laser detuning Δ_1 is greater than the Doppler width, but the Rabi frequency Ω is much smaller than the Doppler width, the qualitative gain and/or absorption features for a homogeneous Λ system are preserved in a Doppler-broadened Λ system. Again, the dominant probe absorption occurs at $\Delta=0$, which is the line center of the probe transition $|3\rangle\leftrightarrow|2\rangle$. The probe spectral feature at $\Delta=\Omega'=[\Delta_1^2+\Omega^2]^{1/2}\approx\Delta_1(\Omega\ll\Delta_1)$ can vary from gain to absorption and change the line shape from dispersive to absorptive, depending on the coupling-laser detuning Δ_1. As shown in Fig. 5, with $\Delta_1=200\gamma_{32}$, the probe laser experiences absorption at $\Delta=\Omega'\approx\Delta_1=200\gamma_{32}$; with $\Delta_1=250\gamma_{32}$, the probe absorption and/or gain spectrum exhibits a dispersive line shape at $\Delta=\Omega'\approx\Delta_1=250\gamma_{32}$; with $\Delta_1=300\gamma_{32}$, the probe laser experiences amplification at $\Delta=\Omega'\approx\Delta_1=300\gamma_{32}$. The near cancellation of the Doppler shifts for the probe transition $|2\rangle\leftrightarrow|3\rangle$ and the coupling transition $|1\rangle\leftrightarrow|3\rangle$ results in a sub-Doppler linewidth in the probe gain and/or absorption feature at $\Delta=\Omega'$. As the pump detuning Δ_1 approaches zero, the probe absorption at $\Delta=\Omega'\approx\Delta_1$ is increased and the absorption linewidth also increases.

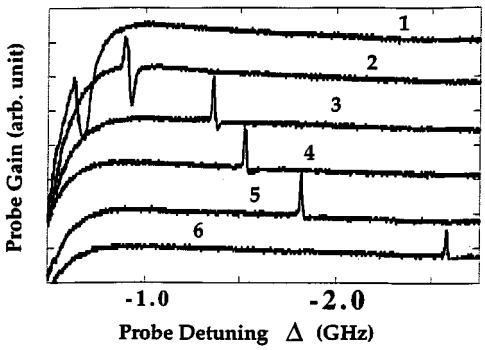

FIG. 6. The measured probe absorption and/or gain spectra near the ^{87}Rb $5S_{1/2}$ $(F=2)\leftrightarrow5P_{3/2}$ transition [the pump laser was tuned to the center of the ^{87}Rb $5S_{1/2}$ $(F=2)\leftrightarrow5P_{3/2}$ transition] for a series of coupling-laser detunings Δ_1 from the ^{87}Rb $5S_{1/2}$ $(F=1)\leftrightarrow5P_{3/2}$ transition (for clarity, different curves have been vertically displaced). When $\Delta_1=-0.7$ GHz, the probe laser is attenuated at $\Delta=-\Omega'\approx-0.7$ GHz (curve 1). When $\Delta_1=-0.9$ GHz, the probe spectrum displays a dispersive line shape at $\Delta=-\Omega'\approx-0.9$ GHz (curve 2). As $|\Delta_1|$ is increased further the normal probe amplification features were observed at $\Delta=-\Omega'\approx\Delta_1$ as shown by curve 3 ($\Delta_1=-1.35$ GHz), curve 4 ($\Delta_1=-1.55$ GHz), curve 5 ($\Delta_1=-1.8$ GHz), and curve 6 ($\Delta_1=-2.6$ GHz). The spectral linewidth gradually narrows down to the natural linewidth. When the detuning Δ_1 is too large, the probe absorption and/or gain feature at $\Delta=-\Omega'\approx\Delta_1$ vanishes.

The theoretical analysis is consistent with our experimental measurement. Shown in Fig. 6 are the measured probe absorption and/or gain spectra near the ^{87}Rb $5S_{1/2}$ $(F=2)\leftrightarrow5P_{3/2}$ transition for a series of pump detunings Δ_1. When the pump detuning $\Delta_1=-700$ MHz, the probe experiences absorption at the probe detuning $\Delta\approx\Delta_1=-700$ MHz (curve 1); when $\Delta_1=-900$ MHz, the probe spectrum exhibits a dispersive line profile at $\Delta\approx\Delta_1=-900$ MHz (curve 2). As the coupling laser was tuned farther away from the transition ^{87}Rb $5S_{1/2}$ $(F=1)\leftrightarrow5P_{3/2}$, the probe laser experiences normal amplification at $\Delta\approx\Delta_1$ as shown by curves 3–6, and the gain linewidth approaches the Rb natural linewidth. When the pump detuning Δ_1 becomes too large, the probe spectral feature at $\Delta\approx\Delta_1$ disappears.

In Fig. 7 we plot the calculated probe gain and/or absorption coefficient ($\mathrm{Im}\rho_{23}$) versus the probe detuning Δ for several values of the coupling Rabi frequency Ω. When the Rabi frequency is too small (the solid curve with $\Omega=\gamma_{32}$), no probe gain can be observed at $\Delta=\Omega'$. As the Rabi frequency Ω of the coupling laser increases, the probe gain appears and increases with Ω. The probe gain is optimized at a moderate Rabi frequency ($\Omega\sim30\gamma$ for the chosen parameters in Fig. 6). Further increase of the coupling-laser intensity reduces the probe gain, and the probe gain line shape changes into a dispersive shape, and eventually evolves into a Doppler-broadened absorption line. This behavior can also be intuitively understood by the dressed-state picture presented in Sec. IV. We have observed such a behavior experimentally. Shown in Fig. 8 are the measured probe gain spectra near the ^{87}Rb $5S_{1/2}$ $(F=2)\leftrightarrow5P_{3/2}$ transition for several coupling-laser intensities while the coupling-laser detuning

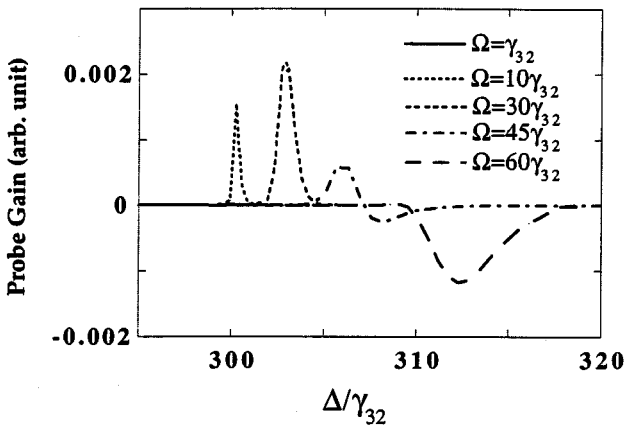

FIG. 7. Calculated probe gain and/or absorption spectra near $\Delta \sim \Omega'$ for several values of the coupling-laser Rabi frequency Ω. The full Doppler width is $100\gamma_{32}$, the coupling-laser detuning $\Delta_1 = 300\gamma_{32}$, and the rest of the parameters are the same as that in Fig. 5. Note that at higher Ω values, the sub-Doppler probe gain at $\Delta = \Omega'$ disappears and is replaced by a broadened absorption feature.

was kept at $\Delta_1 = -1.3$ GHz. The probe gain was observed when the pump power was greater than 2 mW (the estimated pump Rabi frequency is about 30 MHz). As the pump power increases, the probe gain increases accordingly and is maximized at the pump power of about 75 mW (the estimated Rabi frequency is about 150 MHz) as shown by curves 1–3. The probe gain decreases for further increases of the pump power, and the gain profile changes into a dispersive shape as shown by curve 4. At even higher pump intensities, the probe spectral feature at $\Delta \approx \Delta_1$ exhibits a broadened absorption line profile (see curve 5). Overall, the gain spectral feature at

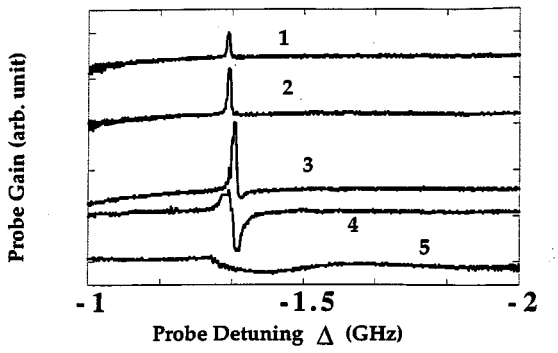

FIG. 8. The measured probe gain spectra near the ^{87}Rb $5S_{1/2}$ $(F=2) \leftrightarrow 5P_{3/2}$ transition with several different coupling-laser intensities (for clarity, different curves have been vertically displaced). The pump laser was tuned to the center of the ^{87}Rb $5S_{1/2}$ $(F=2) \leftrightarrow 5P_{3/2}$ transition and the coupling laser was detuned from the ^{87}Rb $5S_{1/2}$ $(F=1) \leftrightarrow 5P_{3/2}$ transition by $\Delta_1 = -1.3$ GHz. Curves 1–5 correspond to the pump powers 7, 23, 75, 235, and 750 mW, respectively. As the pump intensity increases, the probe spectral line shape changes from amplification to dispersion, then to absorption. The linewidth increases from near the natural linewidth (10 MHz) for the gain feature at lower intensities to a Doppler-broadened width for the absorption feature at higher intensities.

$\Delta = -\Omega' \approx \Delta_1 = -1.3$ GHz exhibits the sub-Doppler line widths that approach the Rb natural linewidth. For example, the measured linewidth for the gain feature in curves 1 and 2 is ~ 10 MHz (about equal to the Rb natural linewidth of 6 MHz after convolution of the laser linewidths of a few MHz for the Ti:sapphire laser and the probe laser).

IV. DRESSED-STATE PICTURE

The observed probe amplification is induced by the two-photon coherence ρ_{12} between the ground states $|1\rangle$ and $|2\rangle$. Although no direct measurement of the population distribution was made, the observed dominant absorption at $\Delta \approx 0$ indicates that there is no population inversion in the bare atomic states. This is consistent with the steady-state solution $\rho_{22} = [(\Gamma + \gamma_{32})/\Gamma]\rho_{33}$. Under the experimental conditions (a moderate coupling laser with large pump detunings Δ_1), the population distribution obeys $\rho_{22} > \rho_{33}$ and $\rho_{11} > \rho_{33}$. Several factors contribute to the inversionless population distribution in the Λ system: First, in general, the effect of the coupling laser (the pump laser) is reversible: it drives the transition $|1\rangle \rightarrow |3\rangle$ ($|2\rangle \rightarrow |3\rangle$) as well as the reverse transition $|3\rangle \rightarrow |1\rangle$ ($|3\rangle \rightarrow |2\rangle$), while the spontaneous decay from $|3\rangle \rightarrow |2\rangle$ and $|3\rangle \rightarrow |1\rangle$ is irreversible [18]; second, the coherent population trapping in the Λ system tends to keeping atoms in the ground states [19]. Perhaps the observed probe amplification by coherence can be best understood by a dressed-state analysis [17,20,21]. The coupling laser drives the Rb $5S_{1/2}$ $F=2$ (state $|1\rangle$) and $5P_{3/2}$ (state $|3\rangle$) states and creates a pair of dressed states $|+\rangle$ and $|-\rangle$ [22]. The energy eigenvalues of the two semiclassical dressed states are

$$E_{\pm} = \frac{\Delta_1}{2} \pm \frac{1}{2}[\Delta_1^2 + 4\Omega^2]^{1/2}. \tag{2}$$

The corresponding semiclassical dressed states are

$$|\pm\rangle = a_{\pm}|1\rangle + b_{\pm}|3\rangle,$$

where the coefficients are given by

$$a_{\pm} = \frac{E_{\pm}}{(E_{\pm}^2 + \Omega^2)}, \quad b_{\pm} = \frac{\Omega}{(E_{\pm}^2 + \Omega^2)}.$$

When the Rabi frequency Ω of the coupling laser is much smaller than the detuning Δ_1, approximately $E_+ \approx \Delta_1$ and $E_- \approx -\Omega^2/\Delta_1$. Then, the dressed state $|+\rangle$ consists largely of the ground state $|1\rangle$ and is shifted in energy by approximately Δ_1 from the bare-state transition; the dressed state $|-\rangle$ consists largely of the excited state $|3\rangle$ and is barely shifted from the bare-state transition. The dressed state picture is drawn in Fig. 9. Figure 9(a) shows the atomic bare-state picture with the coupling laser and the pump laser. Figure 9(b) shows the dressed-state picture without the effect of the pump laser. Here we see that without the pump laser, the population distribution satisfies $\rho_{22} > \rho_{++} > \rho_{--}$ (the atomic population is shown schematically by the number of black dots). The probe gain and/or absorption spectra will show the dominant absorption feature at the dressed-state transition $|2\rangle \rightarrow |-\rangle$ (near the line center of the bare-state transition $\Delta = 0$) and less absorption at the dressed-state transition

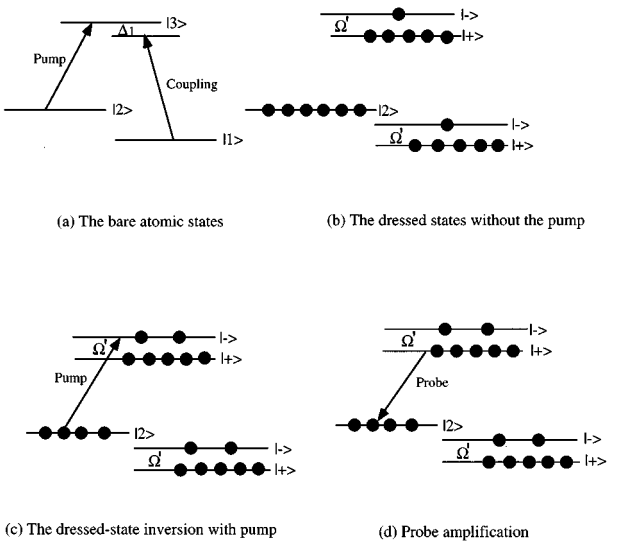

FIG. 9. Interpretation of the probe amplification in terms of the dressed-state picture. (a) The coupled bare atomic states for the three-level Λ system. (b) The coupling laser generates a pair of the dressed states $|+\rangle$ and $|-\rangle$ with the energy separation $\Omega=\sqrt{\Delta_1^2+4\Omega^2}$. Note that with a large detuning Δ_1, the dressed state $|-\rangle$ consists largely of the excited bare state $|3\rangle$ while the dressed state $|+\rangle$ consists largely of the ground bare state $|1\rangle$. If no pump laser is present, the atomic population distribution satisfies $\rho_{22}>\rho_{++}>\rho_{--}$, the probe laser will experiences absorption at the dressed-state transitions $|2\rangle\leftrightarrow|-\rangle$ and $|2\rangle\leftrightarrow|+\rangle$ (the dark dots indicate schematically the atomic population among different states). (c) With the pump laser on and tuned to the transition $|2\rangle\leftrightarrow|-\rangle$ (approximately equal in energy to the bare-state transition $|2\rangle\leftrightarrow 3\rangle$), the atomic population in the bare state $|2\rangle$ will be excited to the dressed state $|-\rangle$, and the population inversion in the dressed-state transition $|+\rangle\rightarrow|2\rangle$ is therefore created. (d) When the probe laser is tuned to the dressed-state transition $|+\rangle\rightarrow|2\rangle$, it will be amplified due to the inverted population in the dressed-state basis, although there is no population inversion in the bare-state basis

.

$|2\rangle\rightarrow|+\rangle$ at the probe detuning $\Delta\approx\Delta_1$ (Autler-Townes doublet). When the pump laser is on and tuned to the bare-state transition (coincided with the dressed-state transition $|2\rangle\rightarrow|-\rangle$ because $E_-\approx-\Omega^2/\Delta_1\sim 0$ for a large detuning Δ_1), some atoms in state $|2\rangle$ are excited to the dressed state $|-\rangle$. When the pump laser is sufficiently strong, the condition of population distribution, $\rho_{++}>\rho_{22}>\rho_{--}$, can be met as shown in Fig. 9(c), and the population inversion between the dressed state $|+\rangle$ and the bare state $|2\rangle$ is created (although there is no population inversion in the bare states $|1\rangle$, $|2\rangle$, and $|3\rangle$). Then the probe laser will be amplified at the inverted transition $|2\rangle\leftarrow|+\rangle$ ($\Delta\approx\Delta_1$) while the dominant probe absorption occurs at the transition $|2\rangle\rightarrow|-\rangle$ at $\Delta\approx 0$ as shown schematically by Fig. 9(d). This is exactly what we observed in the experiment. Therefore, this work represents an observation of light amplification without inversion in the bare states, but with inversion in the dressed states.

The dependence of the probe gain on the coupling-laser detuning Δ_1 and the Rabi frequency Ω can be qualitatively understood as follows. If the incoherent pump field is not too strong, the atoms are heavily populated in the ground states. Therefore the population inversion can only be created at large detunings Δ_1 for the transition between the heavily populated dressed state $|+\rangle$ and the ground state $|2\rangle$ at the probe detuning

$$\Delta\approx\frac{\Delta_1}{2}+\frac{\sqrt{\Delta_1^2+4\Omega^2}}{2}=E_+.$$

For a fixed Rabi frequency Ω, smaller detunings Δ_1 reduces the population imbalance between the dressed states $|+\rangle$ and $|-\rangle$. That is, the atomic population is transferred from the dressed state $|+\rangle$ to the dressed state $|-\rangle$; therefore the population inversion between the dressed state $|+\rangle$ and the ground state $|2\rangle$ ceases to exist at smaller detunings Δ_1. Large detunings Δ_1 lead to more population imbalance between the two dressed states, which is favorable for the probe gain. However, if Δ_1 is too large, the transition probability between the dressed state $|+\rangle$ and the ground state $|2\rangle$ is diminishingly small [9,22], and the probe gain eventually disappears. The evolution of the probe spectral feature at

$$\Delta\approx E_+$$

from absorptive to dispersive, then to amplification, indicates that the population difference $\rho_{++}-\rho_{22}$ changes from smaller than zero to equal to zero, then to greater than zero, as shown in Figs. 5 and 6.

For a given incoherent pump rate Λ and a fixed detuning Δ_1, a sufficiently large Ω value is required to generate a pair of dressed states and induce the coherent probe amplification. However, larger Ω values also reduce the population imbalance between the dressed states $|+\rangle$ and $|-\rangle$, i.e., the atomic population will be transferred from the more heavily populated dressed state to the less populated dressed state ($|+\rangle\rightarrow|-\rangle$ in Fig. 9), and reduces the inverted population $\rho_{++}-\rho_{22}$. When Ω is too large, the population inversion for the dressed-state transition at

$$\Delta\approx E_+$$

eventually ceases to exist, and the probe gain turns into absorption, as shown in Figs. 7 and 8.

V. CONCLUSION

The observed sub-Doppler absorption and/or gain spectrum in the Doppler-broadened Rb system can be qualitatively understood as follows. When the coupling laser and the probe laser propagate in the same direction, the Doppler shifts for the probe transition $|2\rangle\leftrightarrow|3\rangle$ and the pump transition $|1\rangle\leftrightarrow|3\rangle$ are approximately equal, so the two-photon scattering process $|1\rangle\leftrightarrow|3\rangle\leftrightarrow|2\rangle$ is kept on resonance for the Rb atoms with different velocities. Thus the observed probe spectral feature at $\Delta\approx\Delta_1$ (whether it is the gain or absorption) is essentially Doppler-free. This is similar to the Doppler-free two-photon absorption in a vapor cell where a counterpropagating beam configuration has to be applied, and to the recently observed electromagnetically induced

transparency in a Doppler-broadened atomic sample [23,24]. Note that in a Λ atomic system, the coupling laser and the probe laser have to propagate in the same direction to cancel out the Doppler shift. Normally, one would expect that in order to observe the probe gain in a Doppler-broadened system, the Rabi frequency of the coupling laser has to be greater than or comparable to the Doppler width [15,25]. However, the near cancellation of the Doppler shift in the Rb Λ system significantly enhances the probe gain and makes the observation of the probe amplification possible with a low-power coupling laser.

It should be noted that Kumar and Shapiro observed the Raman lasing in sodium *D* lines [26]. Their experiment was carried out in a collision-broadened vapor cell and the Rabi frequency of their pump laser (intensity about 40 W/cm^2) is comparable to the Doppler width. Our experiment was carried out in an essentially collision-free environment and the Rabi frequency of the coupling laser is much smaller than the Doppler width. When the Rabi frequency is comparable to the Doppler width, no gain was observed in our experiment. The major difference of their work from the present work is that for their experimental observation, no population in the excited state $|3\rangle$ is required, and therefore no additional pump from state $|2\rangle$ to state $|3\rangle$ is necessary, while in our experiment, real atomic population in the excited state $|3\rangle$ is required (although no population inversion is needed). Therefore a pump laser is required to excite the atoms to the excited state $|3\rangle$; otherwise, only probe attenuation can be observed. The critical role of the pump laser exciting the atoms to the upper state $|3\rangle$ may be masked by the closeness in energy between states $|1\rangle$ and $|2\rangle$ in the Rb system (the separation is only ~ 3 GHz). However, the usefulness of a Λ system driven by an off-resonant coupling laser in obtaining light amplification is not limited to the Λ system with close-by states $|1\rangle$ and $|2\rangle$. A suitable Λ system driven by an off-resonant pump laser in other atomic species can certainly be used to realize the situation in which the transition frequency between states $|2\rangle$ and $|3\rangle$ is far greater than that between states $|1\rangle$ and $|3\rangle$. Then LWI in the Λ system driven by an off-resonant pump laser can be used to obtain higher lasing frequencies with the help of a lower-frequency coupling laser. Now the role of the pump laser is more clearly exposed because it has to be there to excite the atoms to the excited state (for real applications, the control laser should be replaced by some realistic incoherent pump method). We note that in this situation, the sub-Doppler nature of the probe gain will be diminished and the probe gain will be reduced, but the probe gain will not vanish as shown by Fig. 4 for the calculation of a general Λ system.

In summary, we have observed steady-state, Doppler-free amplification of a weak probe laser without population inversion in the bare states in a coherently pumped, Doppler-broadened Λ-type Rb atomic system. The linewidth of the gain spectral feature approaches the Rb natural linewidth. The probe amplification occurs in a regime where the Rabi frequency of the coupling laser is much smaller, but the coupling-laser detuning is greater, than the Doppler width. The observed light amplification without population inversion in the bare states can be understood in terms of a physical picture of the dressed-state population inversion. A theoretical analysis based on a three-level Λ-type system has been presented and qualitative agreement between the theoretical calculation and experimental measurements has been achieved. It should be noted that the Rb D_2 transitions possess hyperfine structures with magnetic sublevels, so it is not a simple three-level system. However, such simplifying assumptions do provide a reasonably good approximation for the treatment of the Rb system and have been effectively employed in the past on similar systems [15,23–25].

Note added in proof. Recently, realization of LWI oscillators has been reported [27,28].

ACKNOWLEDGMENTS

We thank K. Hardy and J. Sheldon for useful discussions. This work was supported in part by Research Corporation and the U.S. Army Research Office.

[1] S. E. Harris, Phys. Rev. Lett. **62**, 1033 (1989).
[2] O. Kocharovskaya, Phys. Rep. **219**, 175 (1992).
[3] M. O. Scully, Phys. Rep. **219**, 191 (1992).
[4] V. G. Arkhipkin and Yu. I. Heller, Phys. Lett. A **98**, 12 (1983).
[5] G. S. Argarwal, S. Ravi, and J. Cooper, Phys. Rev. A **41**, 4721 (1990).
[6] A. Lyras, X. Tang, P. Lambropoulos, and J. Zhang, Phys. Rev. A **40**, 4131 (1989).
[7] D. Grandclement, G. Grynberg, and M. Pinard, Phys. Rev. Lett. **59**, 44 (1987).
[8] G. Khitrova, J. F. Valley, and H. M. Gibbs, Phys. Rev. Lett. **60**, 1126 (1988).
[9] A. Lezama, Y. Zhu, M. Kanskar, and T. W. Mossberg, Phys. Rev. A **41**, 1576 (1990).
[10] J. Y. Gao *et al.*, Opt. Commun. **93**, 323 (1992).
[11] A. Nottelman, C. Peters, and W. Lange, Phys. Rev. Lett. **70**, 1783 (1993).
[12] E. S. Fry *et al.*, Phys. Rev. Lett. **70**, 3235 (1993).
[13] W. van der Veer *et al.*, Phys. Rev. Lett. **70**, 3243 (1993).
[14] L. M. Narducci *et al.*, Opt. Commun. **86**, 324 (1991).
[15] J. A. Kleinfeld and A. D. Streater, Phys. Rev. A **49**, R4301 (1994).
[16] A. Imamoglu, J. E. Field, and S. E. Harris, Phys. Rev. Lett. **66**, 1154 (1991).
[17] For a comparison of incoherent and coherent excitation, see G. A. Wilson, K. K. Meduri, P. Sellin, and T. W. Mossberg, Phys. Rev. A **50**, 3394 (1994).
[18] Under certain conditions, population inversion may occur in doubly pumped *V* and Ξ systems. See K. K. Meduri, G. A. Wilson, P. B. Sellin, and T. W. Mossberg, Phys. Rev. Lett. **77**, 4311 (1993), and R. W. Whitley and C. R. Stroud, Jr., Phys. Rev. A **14**, 1498 (1976).
[19] R. M. Whitley and C. R. Stroud, Jr., Phys. Rev. A **14**, 1498 (1976); G. Alzetta *et al.*, Nuovo Cimento B **36**, 5 (1976).
[20] G. B. Prasad and G. S. Agarwal, Opt. Commun. **86**, 409 (1991).

[21] Y. Zhu, Phys. Rev. A **45**, R6149 (1992).
[22] C. Cohen-Tannoudji, in *Frontiers in Laser Spectroscopy*, edited by R. Balian, S. Haroche, and S. Liberman (North Holland, Amsterdam, 1977).
[23] M. Xiao, Y. Li, S. Jin, and J. Gea-Banacloche, Phys. Rev. Lett. **74**, 666 (1995); J. Gea-Banacloche, Y. Li, S. Jin, and M. Xiao, Phys. Rev. A **51**, 576 (1995).
[24] R. R. Moseley, S. Shepherd, D. J. Fulton, B. D. Sinclair, and M. H. Dun, Phys. Rev. Lett. **74**, 670 (1995).
[25] M. T. Gruneisen, K. R. MacDonald, and R. W. Boyd, J. Opt. Soc. Am. B **5**, 123 (1987).
[26] P. Kumar and J. Shapiro, Opt. Lett. **10**, 226 (1985).
[27] A. S. Zibrov *et al.*, Phys. Rev. Lett. **75**, 1499 (1995).
[28] G. Welch *et al.* (unpublished).